

# Optimization of the Efficiency in a Syngas Powered SI Engine through Numerical Studies Related to the Geometry of the Combustion Chamber

Carmine Caputo<sup>a,b,c</sup>, Daniele Cirillo<sup>a</sup>, Michela Costa<sup>b</sup>, Maurizio La Villetta<sup>a</sup>, Gaia Martoriello<sup>a,b,d</sup>, Daniele Piazzullo<sup>b,\*</sup>, Raffaele Tuccillo<sup>d</sup>

<sup>a</sup>CMD S.p.A., Dipartimento di Ricerca e Sviluppo, Via Pacinotti 2, 81020 S. Nicola La Strada (Caserta), Italy

<sup>b</sup>CNR – Istituto Motori, Dipartimento di Ingegneria, Viale Marconi, 4, 80125 Naples, Italy

<sup>c</sup>Università degli Studi di Tor Vergata, Dipartimento di Ingegneria, Via del Politecnico, 1, 00133 Rome, Italy

<sup>d</sup>Università degli Studi di Napoli “Federico II”, Dipartimento di Ingegneria Industriale, Via Claudio, 21, 80125 Naples, Italy  
[d.piazzullo@im.cnr.it](mailto:d.piazzullo@im.cnr.it)

The combustion process occurring in an alternative Spark Ignition (SI) engine powered with bio-syngas from biomass gasification was previously studied by authors through the development of two different numerical models: a 0-1D model developed in the GT-Suite® environment, aimed at gaining a first look upon the main features of the heat release by the syngas and engine performances; a 3D Computational Fluid Dynamics (CFD) model developed within the AVL Fire™ software reproducing the engine combustion cycle within a Reynolds Averaged Navier Stokes (RANS) schematization and employing a detailed chemical reaction mechanism to highlight the interaction between the fluid dynamics and the kinetics of the specific biofuel oxidation chain. The numerical results were validated with respect to experimental measurements in a baseline condition, where the presence of a relatively high amount of CO in the exhaust gases was noticed as related to an engine low combustion efficiency, mainly due to the peripheral spark plug position that determines the persistence of residual gases on the opposite side of the combustion chamber wall.

The proposed work presents a numerical analysis made through the developed models on the effects of proper changes in the spark plug position. A multi-objective optimization problem is conducted also by varying the Start of Spark (SOS) and the mixture air-to-fuel ratio with the aim of reducing the engine environmental impact without affecting its performances. A centrally mounted spark, along with a correct calibration of the SOS and mixture ratio, allows a reduction of more than 90% of CO emission with respect to the baseline condition without penalizing the engine brake power and efficiency.

## 1. Introduction

A promising alternative source to traditional fuels is syngas deriving from biomass gasification (Shah et al., 2010). This last is a well-known thermochemical process for the valorisation of organic materials and residual wastes to produce a gaseous fuel that can be used for cogenerative purposes. A considerable reduction of the emitted CO<sub>2</sub> can be achieved, especially if a local supply chain is included to produce, process and valorise the available biomass in rural areas (RaF Italia, 2019). Due to the fluctuation in syngas composition, there are still some inefficiencies when exploited in alternative engines. Syngas has a lower energy density, heating value and volumetric efficiency than gasoline (Costa et al., 2017), mainly due to the presence of light species in its composition. A low combustion efficiency is generally expected, leaving the presence of residual unburned gases as CO in the combustion chamber (Caputo et al., 2019).

Within the field of thermal engines, finding measures to reduce pollutant emission while simultaneously keeping high thermal efficiency is a challenging task. Model-based optimization represents a useful tool to determine cheap and fast results with an acceptable degree of accuracy once reliable numerical models are available.

The performances and emissions deriving from a SI cogenerative engine powered with bio-syngas was previously studied by authors through the development and validation of two different numerical models characterized by an increased level of detail (Caputo et al., 2019), whose results enlightened the presence of a relatively high amount of CO in the exhaust gases due to a peripheral spark plug position. This circumstance was also found on the experimental side of a campaign properly executed on a real biomass powered CHP plant of the micro-scale power (Caputo et al., 2019). In present paper a multi-objective optimization problem is conducted by varying the spark plug position, the Start of Spark (SOS) and the mixture air-to-fuel ratio with the aim of enhance the engine combustion efficiency without burdening its environmental impact.

## 2. Experimental layout

The considered SI engine is a 3.0L GM Vortec I-4 engine, part of a CHP unit combining a downdraft gasifier and a syngas cleaning device, this last implemented to guarantee syngas pureness through a process of cleaning, cooling and filtering (Caputo et al., 2019). The ICE is naturally aspirated 4-cylinder in-line, liquid-cooled, powered by syngas. It is equipped with an oil tank-refilling pump and oil filter for continuous operation. Further characteristics are reported in Table 1.

Table 1. Engine geometrical characteristics (Caputo et al., 2019).

Displacement	3000 cc
Compression Ratio	10.5
Bore x Stroke [mm]	101.60 x 91.44
Connecting Rod [mm]	203.2
Intake Valve Open (IVO)	101°
Intake Valve Close (IVC)	256°
Exhaust Valve Open (EVO)	470°
Exhaust Valve Close (EVC)	659°
Maximum intake/exhaust valve open	11.25 mm
RPM	1500

## 3. 0-1D Model Development and Validation

A zero-one dimensional (0-1D) model in the GT- Power™ environment is developed to reproduce the complete engine cycle under syngas feeding. The model solves the Navier-Stokes equations in a one-dimensional framework, as each pipe and flow split is discretized into many sub-volumes to better approximate bends or restrictions. All the engine components are modelled, from the intake to the exhaust ducts, considering the throttle, the valves and the cylinders. The combustion model adopted is the *EngCylCombSITurb*, a predictive approach that allows the evaluation of the direct influence of the syngas composition over the flame speed and combustion propagation (Hernandez et al., 2005). This approach is preferred to the more classical Wiebe function (Heywood, 1988), where the fuel burned mass fraction is defined through a sigmoid-like function, as it is indeed validated for fossil fuels but it fails when a non-traditional fuel (as syngas from biomass gasification) is considered. The model validation is performed with reference to a *baseline* condition, where syngas deriving from gasification of woodchip is exploited in the SI engine under stoichiometric conditions at a SOS of 34° Before Top Dead Center (BTDC). The measured syngas composition is reported in Table 2. Further details about the model and about the initial and boundary conditions can be found in (Caputo et al., 2018; Caputo et al., 2019).

Table 2. Mass fractions of the species composing the syngas under study (Caputo et al., 2019).

H <sub>2</sub>	1.18%
CO	20.02%
CH <sub>4</sub>	1.14%
CO <sub>2</sub>	14.9%
C <sub>2</sub> H <sub>6</sub>	0.47%
N <sub>2</sub>	60.21%
H <sub>2</sub> O	2.09%
$\alpha_{ST}$	1.185
LHV [MJ/kg]	4.22

Figures 1a,b show the comparison between numerical and experimental results in terms of pressure cycle and CO emissions, depicted at the exhaust. The 0-1D model is found to be able to model the syngas combustion process in both the compression and expansion phases, with an error percentage equal to 6% on the CO emission, thanks to the implementation of a precise combustion model able to evaluate the laminar flame speed evolution as a function of the gaseous fuel composition. Further comparisons are reported in (Caputo et al., 2019).

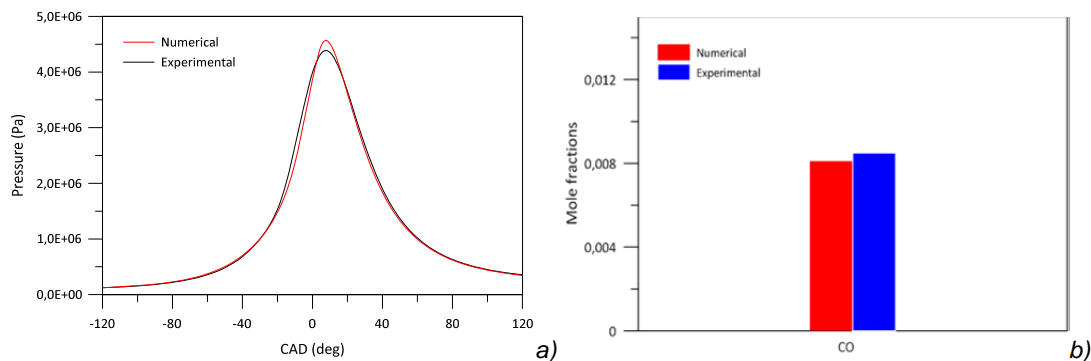


Figure 1. Comparison of a) the pressure cycle and b) the CO emissions between the 1D model and experimental data.

#### 4. 3D CFD Model Development and Validation

The 3D CFD numerical model is developed in the AVL Fire™ environment, where the moving numerical grid of the complete operating cycle is generated through the Fame Engine Plus tool.

The software includes a fluid dynamic solver based on the finite volume method, solving the balance equations in a Eulerian framework. The turbulent flow field is reproduced within a Reynolds Averaged Navier Stokes (RANS) approach basing on the  $k$ - $\zeta$ - $f$  model (Durbin, 1991). The combustion process is modelled using the General Gas Phase Reaction approach through the implementation of the detailed kinetic mechanism GRI-Mech 3.0 (Smith et al., 1999), for a predictive simulation of chemical processes involving the use of syngas (Piazzullo et al., 2018). Details about the cell dimension belonging to the numerical grid and about the set initial and boundary conditions as derived from an experimental campaign, can be found in (Caputo et al., 2019). The comparison between the experimental and numerical pressure cycles and Rates of Heat Release (ROHR) is shown in Figure 2.a. The compression phase is well captured, while the expansion phase is slightly overestimated of about the 6%. The comparison between the measured and calculated mole fractions at the exhaust of the species CO, CO<sub>2</sub> and H<sub>2</sub>O are instead shown in Figure 2.b. CO emissions are numerically unpredicted with an error percentage less than 11%.

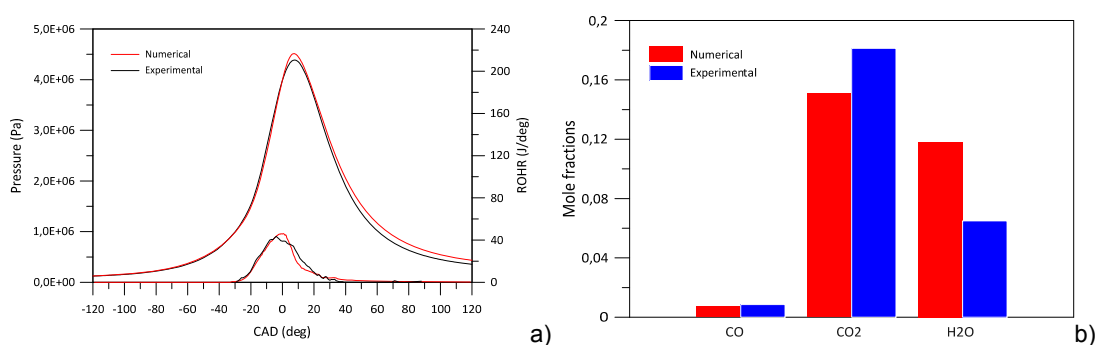


Figure 2. Comparison of a) the pressure cycle and ROHR and b) the CO, CO<sub>2</sub> and H<sub>2</sub>O emissions between the 3D CFD simulation and experimental data for a SOS 34° BTDC, stoichiometric equivalence ratio (Caputo et al., 2019).

#### 5. Combustion Efficiency Optimization through a Parametric Study of the Spark Plug Position

The relatively high amount of CO measured in the exhaust gases during the experimental campaign was also noticed from the results of both the 0-1D and 3D CFD models. These last enlightened how this low

combustion efficiency is mainly related to the peripheral spark plug position that determines the persistence of residual gases on the opposite side of the combustion chamber wall (Caputo et al., 2019). Therefore, a parametric analysis is first conducted in the 0-1D model to study the effects of the spark plug position inside the combustion chamber over the combustion efficiency and over the residual amount of CO at the EVO. This simulation is performed under the same initial and boundary conditions imposed in the baseline condition, thus by burning the air-syngas mixture in stoichiometric ratio at a SOS of 34° BTDC and by varying the dimensionless spark position. Figures 3a.b show the results in terms of the emitted amount of CO, the Indicated Mean Effective Pressure (IMEP) and the combustion barycentre (the angle where the fuel Burned Mass Fraction (BMF) reaches the 50%) as the spark plug is shifted towards the centre. The results are plotted against the dimensionless position of the spark in the combustion chamber, in a range between 1 (original spark plug position) and 0 (spark plug in the combustion chamber centre). As the spark is shifted along the combustion chamber axis towards the centre, a gradual reduction of the CO emitted can be noticed, up to a 25.6% less when the spark is placed in the combustion chamber centre (Figure 3.a) where the highest combustion efficiency is reached. However, the power produced by the engine also reduces, as noticed by the IMEP variation in Figure 5.b, as the central position of the spark determines faster combustion speed with a consequent shift of the early combustion development during the compression phase (Figure 3.b).

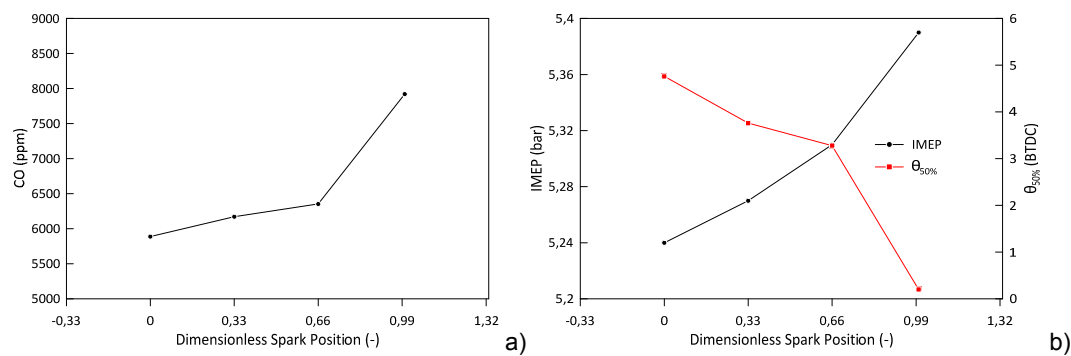


Figure 3. Comparison of the 0-1D simulation results in terms of a) CO emitted and b) IMEP and combustion barycentre variations the spark plug is shifted from the original to a central position in the combustion chamber.

Therefore, a multi-objective optimization problem is formulated also accounting a simultaneous variation of the SOS and the spark position. As the mixture air-to-fuel ratio also plays a fundamental role, this variable is also considered with the aim of finding the operative condition at which the engine operates with few CO emissions, while maintaining high efficiency (the maximum IMEP reduction was set at 5%) when the spark is placed in a central position. This optimization problem is performed in the ModeFrontier™ software through a previously validated methodology available in (Costa et al., 2019), where an approach based on the Non-dominated Sorting Genetic Algorithm (NSGA-II) code algorithm finds the optimum condition in a defined Design Of Experiment (DOE), where the SOS is varied between 24° and 36° BTDC while the air-to-fuel ratio ranges between 0.9 and 1.1. The optimum condition with a central spark position is found when the engine operates at a SOS of 30° BTDC at an air-to-fuel ratio equal to 1.06. The results of the 0-1D simulation in terms of produced IMEP and emitted CO between the baseline, the central spark and the optimum conditions are reported in Table 3, where a substantial reduction of the CO emitted equal to the 51.7% can be noticed for the last analysed case, despite the same power produced by the engine with respect to the original configuration. For the sake of clarity, it must be said that the initial amount of CO trapped in the combustion chamber for the optimum condition is just the 2.4% lower than the one characterising the baseline condition, thus the percentual variation reported in the last column of Table 3 can be still considered as valid.

Table 3. Comparison of the engine performances resulting from the 0-1D simulation between the baseline condition with lateral spark, baseline condition with central spark and optimum condition achieved with central positioned spark.

	Baseline	Central-Spark	Deviation (%)	Optimum	Deviation (%)
IMEP (bar)	5.39	5.23	-2.9	5.32	1.3
CO (ppm)	7921	5887	-25.6	3822	-51.7

Lastly, a newly generated numerical grid, characterised by a symmetrical configuration with the spark plug placed in a central position, is generated to perform two 3D CFD simulations under both the central-spark and optimum operative conditions, with the aim of comparing the flow-field evolution, the chemical-fluid dynamic

interaction and their influence over the combustion propagation with respect to the previous baseline condition. The newly generated combustion chamber is characterised by the same compression ratio, trapped mass and displacement of the original configuration in order to perform a correct comparison and is shown in Figure 4 at the TDC position. The comparison of the simulated pressure cycle evolution between the 0-1D and the 3D CFD simulation is reported in Figures 5a,b for both the central-spark and optimum operative conditions. The agreement is considered satisfactory in both the compression and combustion phase, as well as in the position of the peak of pressure, despite a numerical overestimation still achieved during the expansion phase achieved by the CFD simulation (pressure around 10% higher). Figures 6 shows the comparison among the baseline and operative cases studied of the CO mass fraction inside the combustion chamber at different crank angle degrees on a plane passing through the spark plug.



Figure 4. Numerical grid of the combustion chamber with spark plug placed in a central position.

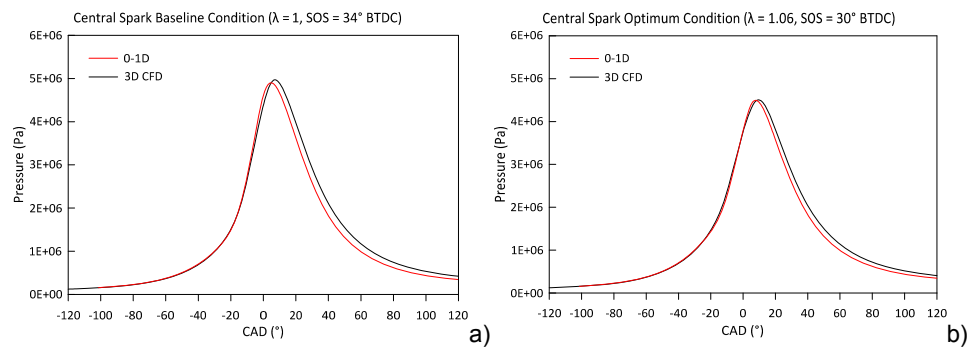


Figure 5. Comparison of the pressure cycles achieved from the 0-1D and 3D CFD simulations for the a) baseline central-spark and b) optimum operative condition.

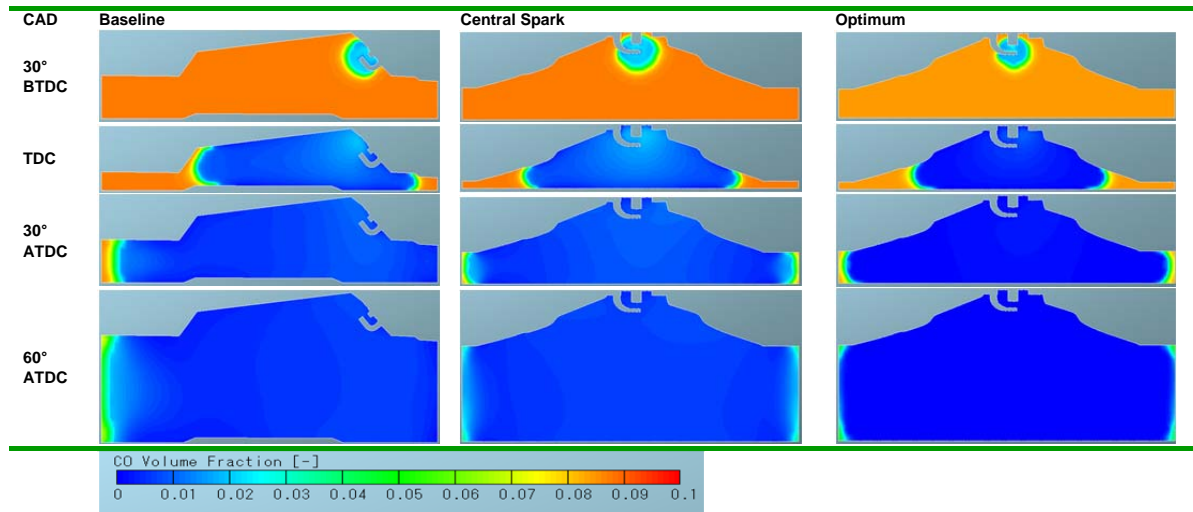


Figure 6. Comparison of the CO volume fraction consumption at different crank angles from the 3D CFD simulations in a plane passing through the spark plug between the baseline condition with lateral spark, baseline condition with central spark and optimum condition achieved with central positioned spark.

This evolution of the CO volume fraction is also reported in Figure 7, where a faster and more efficient combustion can be clearly depicted by the rate of consumption of this species. However, the comparison of the CO mass fraction emitted by the engine among the three cases in Table 4 shows an overestimation with respect to the values resulting from the 0-1D simulation. This can be attributed to the higher values of pressure and temperature achieved during the expansion phase, as shown in Figure 5, that favour the oxidation of this specie.

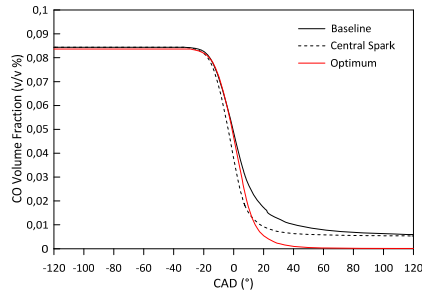


Figure 7. Comparison of the CO volume fraction consumption from the 3D CFD simulations between the baseline condition with lateral spark, baseline condition with central spark and optimum condition achieved with central positioned spark.

Table 4. Comparison of the CO volume fraction achieved from the 3D CFD simulation between the baseline condition with lateral spark, baseline condition with central spark and optimum condition achieved with central positioned spark.

	Baseline	Central-Spark	Deviation (%)	Optimum	Deviation (%)
CO (ppm)	5714.6	5331.4	-7.7	514.3	-91

## 6. Conclusions

A comprehensive multi-objective optimization problem, formulated with reference to a real alternative engine under bio-syngas feeding by varying the spark plug position, SOS and the mixture air-to-fuel ratio, is conducted by using a validated 0-1D model, with the aim of increasing the engine combustion efficiency by reducing the CO emissions at the exhaust. The optimum condition is found when the spark plug is placed in a central position, at a SOS of 30° BTDC and an air-to-fuel ratio equal to 1.06, giving an expected CO reduction equal to 51.7% with respect to the original baseline condition. The results are then confirmed by 3D CFD simulations performed on a newly generated numerical grid with the spark placed in a central position, where a faster consumption of the CO volume fraction and a more efficient combustion are evident in the optimal condition. However, the predicted CO reduction is overestimated with respect to the trend depicted from the 0-1D model, as the pressure evolution depicted by the 3D CFD model is higher than the measured one. A possible future solution to achieve a better agreement during the expansion phase is by employing different detailed mechanism for syngas combustion.

## References

- Caputo C., Cirillo D., Costa M., Di Blasio G. et al., 2019, Multi-Level Modeling of Real Syngas Combustion in a Spark Ignition Engine and Experimental Validation, SAE Technical Paper 2019-24-0012.
- Caputo C., Cirillo D., Costa M., La Villetta M. et al., 2018, Numerical Analysis of a Combined Heat and Power Generation Technology from Residual Biomasses, Journal of Energy and Power Engineering, 12, 300-321.
- Costa M., La Villetta M., Massarotti N., 2017, Numerical analysis of a compression ignition engine powered in the dual-fuel mode with syngas and biodiesel, Energy, 137, 69-979.
- Costa M., Rocco V., Caputo C., Cirillo D. et al., 2019, Model based optimization of the control strategy of a gasifier coupled with a spark ignition engine in a biomass powered cogeneration system, Applied Thermal Engineering, 114083.
- Durbin P.A., 1991, Near-wall turbulence closure modeling without “damping functions”, Journal of Theoretical and Computational Fluid Dynamics, 3, 1-13.
- Hernandez J.J., Lapuerta M., Serrano C., Melgar A., 2005, Estimation of the laminar flame speed of producer gas from biomass gasification, Energy & fuels, 19(5), 2172-2178.
- Heywood J.B., (Ed.) 1988, Internal combustion engine fundamentals, McGraw Hill.
- Piazzullo D., Costa M., Petranovic Z., Vujanovic M. et al., 2018, CFD Modelling of a Spark Ignition Internal Combustion Engine Fuelled with Syngas for a mCHP System, Chemical Engineering Transactions, 65, 13-18.
- Rapporto sullo stato delle foreste e del settore forestale in Italia 2017-2018, RaF Italia, available at: <https://www.reterurale.it/RAFITALIA>, 2019.
- Shah A., Srinivasan R., To S. D. F., Columbus E.P., 2010, Performance and emissions of a spark-ignited engine driven generator on biomass-based syngas, Bioresource technology, 101, 4656-4661.
- Smith G.P., Golden D.M., Frenklach M., Moriarty N.W., 1999, GRI-Mech 3.0, Berkley University.